Paper

Propagation characteristics of single-polarization optical fibers with the cross section of arbitrary shape

Non-member Shin-ichi Furukawa (Sano international information junior college)
Non-member Masayuki Saitou (College of science and technology, Nihon University)
Member Takashi Hinata (College of science and technology, Nihon University)

In this paper, propagation characteristics of a single polarization optical fiber with the cross section of arbitrary shape are numerically studied by applying the circular Fourier expansion method. Firstly, for a single elliptical core fiber, an accuracy of the circular Fourier expansion method is discussed by comparing to a rigorous analysis method using Mathieu functions. Secondly, as an application of the circular Fourier expansion method, a single polarization optical fiber composed of an elliptic core with round shoulder and fluctuations in the pit of circular periphery is designed so as to satisfy the zero total dispersion at wavelength $1.55\mu m$ and is discussed for the single polarization bandwidth and the wavelength sensitivity of the total dispersion. These results are compared with the case of the single polarization optical fiber without round shoulder and fluctuations.

Keywords: single polarization optical fiber, total dispersion, circular Fourier expansion method

1. Introduction

Single-polarization optical fibers (SPF's) are useful for a long-distance transmission line in the large-capacity optical communication systems[1]. We have analyzed propagation characteristics of a SPF composed of a core, cladding, and hollow pits of the ellipse and/or the circle[2]~[5]. The point matching method (PMM) was taken for the numerical technique. Whereas PMM is quite reliable for almost SPF without stress applying area, an application to SPF with complicated profiles such as non-uniform refractive index profiles will be difficult. As such case, SPF with round shoulder and the refractive index fluctuations, which cause in a production process, is supposed. In our earlier work, the influence of round shoulder and fluctuations was analytically found for single mode fibers with axially symmetric structure[6]. In this paper, the circular Fourier expansion method (CFEM) proposed by C.Vassalo[7] are taken to attain the propagation characteristics of SPF. This method can be adapted to the optical waveguides with radial and angular non-uniform refractive index profiles in a homogeneous cladding (see Fig.1). In Ref.(7), optical waveguides composed of various refractive index profiles are not studied and the accuracy of the results are not investigated.

In the numerical analysis, SPF composed of an elliptic core with round shoulder and fluctuations in the pit of circular periphery (non-ideal SPF, see Fig.2(b)) are investigated for structure parameters satisfying the zero total dispersion, the

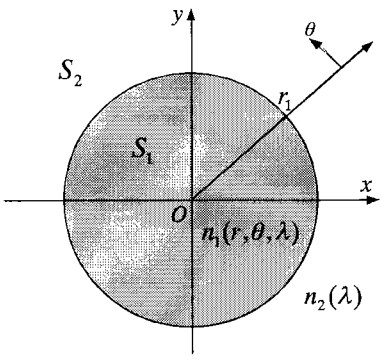

Fig.1 The coordinate systems

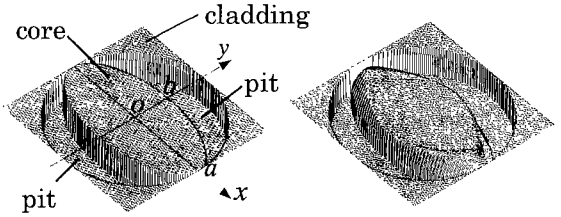

(a) ideal SPF (b) non-ideal SPF

Fig.2 Refractive index profiles of ideal SPF and non-ideal SPF

single polarization bandwidth, and the wavelength sensitivity of the total dispersion. These results are compared with the SPF without round shoulder and fluctuations in Ref.(3) (ideal SPF, see Fig.2 (a)). Furthermore, an accuracy of CFEM is also discussed for the case of the single elliptical core fiber obtained of the rigorous propagation constants.

2. Formulation

The cross section of the fiber with arbitrary refractive index profile is shown in Fig.1. The cylindrical coordinate system (r,θ,z) are introduced. We shall confine the treatment to waves propagating along the z-axis with the factor $\exp(-j\beta z)$. The harmonic time dependence $\exp(-j\omega t)$ is omitted in the field expression. The cross section of the fiber is divided to two regions of S_1 and S_2 along the r-axis. S_1 is the inhomogeneous area including core, pit, or cladding. S_2 is the homogeneous area of the only cladding. The refractive index in the region S_1 and S_2 is $n_1(r,\theta,\lambda)$ and $n_2(\lambda)$, respectively. Since only symmetrical structure with respect to x-axis is considered throughout this paper, the circular Fourier expansion of the refractive index profile and its reciprocal in the region S_2 are denoted by

$$n_1^2(r,\theta,\lambda)=\sum_{p=0}^{N}\varepsilon_p(r,\lambda)\cos p\theta \tag{1}$$

$$1/n_1^2(r,\theta,\lambda)=\sum_{p=0}^{N}\varepsilon_p^{-1}(r,\lambda)\cos p\theta \tag{2}$$

where $\varepsilon_p(r,\lambda)$ and $\varepsilon_p^{-1}(r,\lambda)$ are the Fourier coefficients. The electromagnetic fields in the region $S_\ell(\ell=1,2)$ can be also separated into the even modes and into the odd modes. The electromagnetic fields of the even modes in the region S_ℓ can be expressed by the circular Fourier expansion as follows:

$$E_z^{(\ell)}(r,\theta)=j\sum_{p=0}^{N}E_{zp}^{(\ell)}(r)\cos p\theta \tag{3}$$

$$H_z^{(\ell)}(r,\theta)=j\sum_{p=1}^{N}H_{zp}^{(\ell)}(r)\sin p\theta \tag{4}$$

$$E_\theta^{(\ell)}(r,\theta)=\sum_{p=1}^{N}E_{\theta p}^{(\ell)}(r)\sin p\theta \tag{5}$$

$$H_\theta^{(\ell)}(r,\theta)=\sum_{p=0}^{N}H_{\theta p}^{(\ell)}(r)\cos p\theta \tag{6}$$

$$E_r^{(\ell)}(r,\theta)=\sum_{p=0}^{N}E_{rp}^{(\ell)}(r)\cos p\theta \tag{7}$$

$$H_r^{(\ell)}(r,\theta)=\sum_{p=1}^{N}H_{rp}^{(\ell)}(r)\sin p\theta \tag{8}$$

where $E_{zp}^{(\ell)}(r)$, $H_{zp}^{(\ell)}(r)$, $E_{\theta p}^{(\ell)}(r)$, $H_{\theta p}^{(\ell)}(r)$, $E_{rp}^{(\ell)}(r)$, and $H_{rp}^{(\ell)}(r)$ are the Fourier coefficients. The odd modes can be analyzed by interchanging sin and cos together with p=0 and p=1. $E_{zp}^{(\ell)}(r), H_{zp}^{(\ell)}(r), E_{\theta p}^{(\ell)}(r), H_{\theta p}^{(\ell)}(r), E_{rp}^{(\ell)}(r)$, and $H_{rp}^{(\ell)}(r)$ in the region S_ℓ are derived from equations (3)-(8) and Maxwell's equations. The Fourier coefficients of the electromagnetic fields in the region S_1 $(r\le r_1)$ are as follows:

$$\left.\begin{aligned}
\frac{d}{dr}E_{zp}^{(1)}(r)&=kZ_0H_{\theta p}^{(1)}(r)-\beta E_{rp}^{(1)}(r)\\
\frac{d}{dr}H_{zp}^{(1)}(r)&=-\frac{k}{Z_0}U_{\theta p}(r)-\beta H_{rp}^{(1)}(r)\\
\frac{d}{dr}E_{\theta p}^{(1)}(r)&=-\frac{1}{r}E_{\theta p}^{(1)}(r)+kZ_0H_{zp}^{(1)}(r)-\frac{p}{r}E_{rp}^{(1)}(r)\\
\frac{d}{dr}H_{\theta p}^{(1)}(r)&=-\frac{1}{r}H_{\theta p}^{(1)}(r)-\frac{k}{Z_0}U_{zp}(r)+\frac{p}{r}H_{rp}^{(1)}(r)
\end{aligned}\right\} \tag{9}$$

$$\left.\begin{aligned}
E_{rp}^{(1)}(r)&=\frac{Z_0}{k}\left[\frac{1}{r}V_{zp}(r)+V_{\theta p}(r)\right]\\
H_{rp}^{(1)}(r)&=\frac{1}{kZ_0}\left[\frac{p}{r}E_{zp}^{(1)}(r)-\beta E_{\theta p}^{(1)}(r)\right]
\end{aligned}\right\} \tag{10}$$

where $U_{zp}(r)$, $U_{\theta p}(r)$, $V_{zp}(r)$, and $V_{\theta p}(r)$ are p-th coefficient of $n_1^2(r,\theta,\lambda)E_z(r,\theta)$, $n_1^2(r,\theta,\lambda)E_\theta(r,\theta)$, $[1/n_1^2(r,\theta,\lambda)]d/d\theta[H_z(r,\theta)]$, and $[1/n_1^2(r,\theta,\lambda)]H_\theta(r,\theta)$, respectively. Z_0 is the wave impedance in free space. The simultaneous ordinary differential equation (9) is calculated by a direct numerical integration method. We implement this computation by 4-th order Runge-Kutta method. For the aim of an efficient numerical analysis, the homogeneous region S_0 is located in the region S_1 correspond to the refractive index profile. The region S_0 has the variable radius r_0 in the range of $0<r_0<r_1$ and the refractive index $n_0(\lambda)$. The Fourier coefficients of the electromagnetic fields in the region $S_0(r\le r_0)$ and S_2 $(r_1\le r)$ can be analytically given by the Bessel function or the modified Bessel function of the first kind and the modified Bessel function of the second kind, respectively[7]. The propagation constants can be computed from the eigenvalue equation which is obtained by imposing the continuity conditions of the boundary at $r=r_0$ and $r=r_1$. The normalized propagation constants of the even and the odd fundamental modes are defined by

$$b_q\triangleq\frac{(\beta_q/k)^2-n_2^2(\lambda)}{n_{\max}^2(\lambda)-n_2^2(\lambda)},\qquad q=e\ \ or\ \ o \tag{11}$$

where $n_{\max}(\lambda)$ is the maximum value of $n_1(r,\theta,\lambda)$. The effective cutoff wavelength λ_{cl} is assumed to be the wavelength at $b_q=10^{-4}$. The single-polarization bandwidth $\delta\lambda$ and the total dispersion S_q are defined by the following equations:

$$\delta\lambda\triangleq|\lambda_{co}-\lambda_{ce}| \tag{12}$$

$$S_q\triangleq\frac{k^2}{2\pi c}\cdot\frac{d^2\beta_q}{dk^2},\qquad q=e\ \ or\ \ o \tag{13}$$

λ_{co} and λ_{ce}:the effective cutoff wavelengths of the even

and the odd fundamental mode, respectively.

β_o and β_e :the propagation constants of the odd and the even fundamental mode, respectively.

c : the velocity of light in the free space.

3. Numerical results

Fig.2(a) is ideal SPF reported in Ref.(3). Fig.2(b) is non-ideal SPF with round shoulder and fluctuations in an elliptical core analyzed in this paper. We assumed that non-ideal SPF of Fig.2(b) are made of the pure silica core, the fluorine doped cladding, and hollow pit. The refractive indices $n_{\max}(\lambda)$ and $n_2(\lambda)$ are given by Ref.(8) as

$$n_{\max}(\lambda) = n_S(\lambda) \tag{14}$$

$$n_2(\lambda) = [n_F(\lambda) - n_S(\lambda)](d_2^F / d^F) + n_S(\lambda) \tag{15}$$

$n_S(\lambda)$:the refractive index of the pure silica.

$n_F(\lambda)$:the refractive index of the fluorine doped silica with 1 mole % doping level of fluorine (d_F =1, d_F : reference doping level).

d_2^F :the doping level of fluorine.

Three-term Sellmeier equations[9] is used as dispersion characteristics of $n_S(\lambda)$ and $n_F(\lambda)$. As an example of round shoulder and fluctuations, $n_1(r,\theta,\lambda)$ of non-ideal SPF is assumed to be expressed by the profile in Ref.(6). A derivation method for the Fourier coefficient of $n_1(r,\theta,\lambda)$ is described in Ref.(7). The relative index difference $\Delta(\lambda)$ between the inhomogeneous core and the cladding are defined by

$$\Delta(\lambda) \triangleq [n_{\max}(\lambda) - n_2(\lambda)] / n_{\max}(\lambda) \tag{16}$$

The $\Delta(\lambda)$ at λ =1.55 μm are simply denoted by Δ. In the results, a is used both the semimajor core radius and the radius of the circular hollow pit. The axis ratio of the elliptical core is denoted by b/a.

The accuracy of the normalized propagation constant b_q and the single-polarization bandwidth $\delta\lambda$ are decided by the truncation number N of the Fourier expansion and the division number M of 4-th order Runge-Kutta. In addition, because S_q is computed by a numerical differentiation method using the three point central difference, the accuracy of this method also depends on the step width h. In the numerical analysis, the relative errors of $\delta\lambda$ and S_q are always kept less than 0.1% by carefully selecting the value of N, M, and h.

For the even fundamental mode of a single elliptical core fiber, Fig.3 shows a comparison of the value of b_e computed by CFEM (solid line) and the true value of b_e computed by the rigorous analysis using Mathieu functions (dotted line) as a function of $1/\lambda$. b/a is varied between 0.2 and 0.9. Fig.4 shows a similar comparison result of prorogation constants b_o for the odd fundamental mode. It is found that b_e and

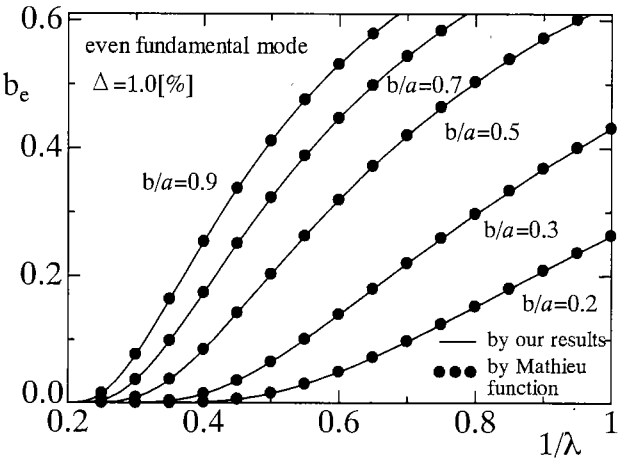

Fig.3 The normarized propagation constant b_e versus $1/\lambda$

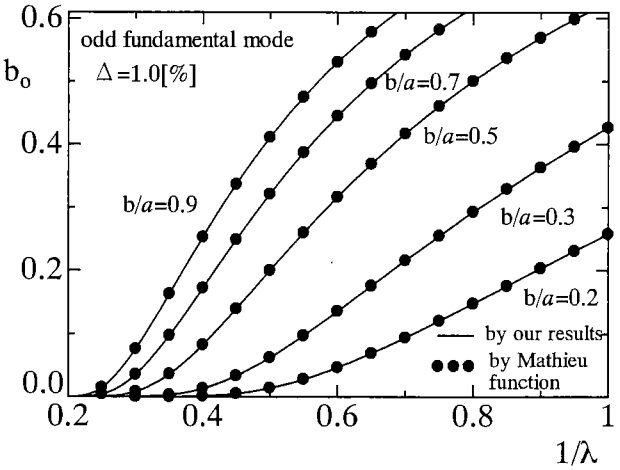

Fig.4 The normarized propagation constant b_e versus $1/\lambda$

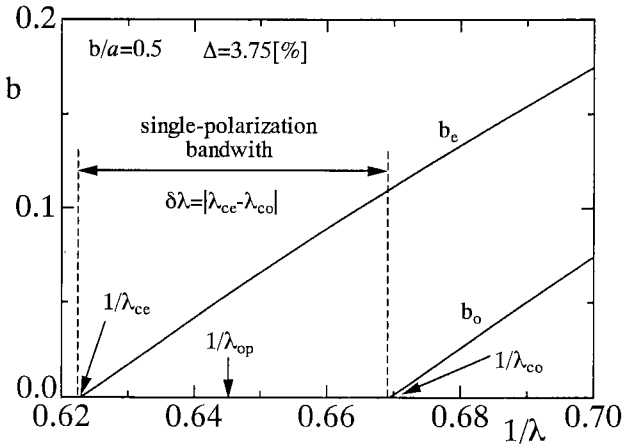

Fig.5 The normarized propagation constant b_e and b_o versus $1/\lambda$

b_o of this paper well agree with the true value.

Fig.5 shows the normalized propagation constants b_e and b_o as a function of $1/\lambda$ for non-ideal SPF. From this figure, the guided mode in the single-polarization bandwidth is the even fundamental mode because $\lambda_{co} < \lambda_{ce}$. Thus, total dispersion is analyzed only for the even fundamental mode. In this paper, the operating wavelength λ_{op} ($\triangleq \lambda_{co} + \delta\lambda/2$) is fixed at 1.55 μm, which gives the lowest transmission loss of silica fibers.

In the following results, $|S_e| \leq 10^{-2} ps/km/nm$ at λ_{op} = 1.55 μm is taken as the zero total dispersion instead of exact zero of S_e.

Fig.6 shows the relative index difference Δ and the semimajor core radius a versus b/a ($0.5 \leq b/a \leq 0.75$) satisfying the zero total dispersion at λ_{op} = 1.55 μm. The solid and broken lines are the results of non-ideal SPF and ideal SPF[3], respectively. Δ and a of non-ideal SPF are different as compared with those of ideal SPF.

Fig.7 shows the single-polarization bandwidth $\delta\lambda$ versus b/a computing by Δ and a designed in Fig.6. The range of b/a and the meaning of the solid and broken lines in Fig.7 are as same as those in Fig.6. $\delta\lambda$ of non-ideal SPF becomes fairly smaller by influence of round shoulder and fluctuations than that of ideal SPF.

Fig.8 shows the total dispersion S_e versus the wavelength λ at b/a =0.5. For a start, ideal SPF is assumed to be designed so as to satisfy the zero total dispersion (see ① in Fig.8). However, if this ideal SPF is caused round shoulder and fluctuations in production process, the zero total dispersion can not be satisfied (see ② in Fig.8). Then, the zero total dispersion is realized by beforehand utilizing Δ, a, and b/a for non-ideal SPF of Fig.6 (see ③ in Fig.8). The wavelength sensitivity $dS_e/d\lambda$ of the total dispersion for non-ideal SPF(③) becomes slightly larger than that for ideal SPF (①).

4. Conclusion

In this paper, the non-ideal SPF composed of an elliptic core with round shoulder and fluctuations in the pit of circular periphery satisfying the zero total dispersion was studied for the single polarization bandwidth and the wavelength sensitivity of the total dispersion. The results were compared with the case of the ideal SPF in Ref.(3). The main results are as follows:

(1)The single-polarization bandwidth $\delta\lambda$ of non-ideal SPF becomes fairly smaller by influence of round shoulder and fluctuations than that of ideal SPF.

(2)We found out the structure parameters for non-ideal SPF that can be satisfied the zero total dispersion by an estima-

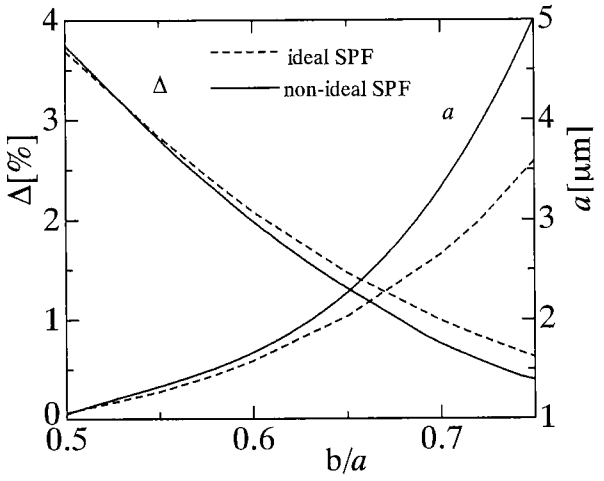

Fig.6 The semimajor radius a and the relative index difference Δ versus b/a

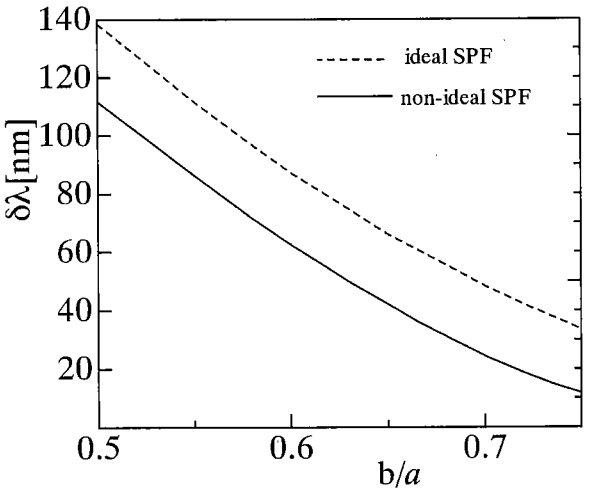

Fig.7 The single polarization bandwidth λ versus b/a

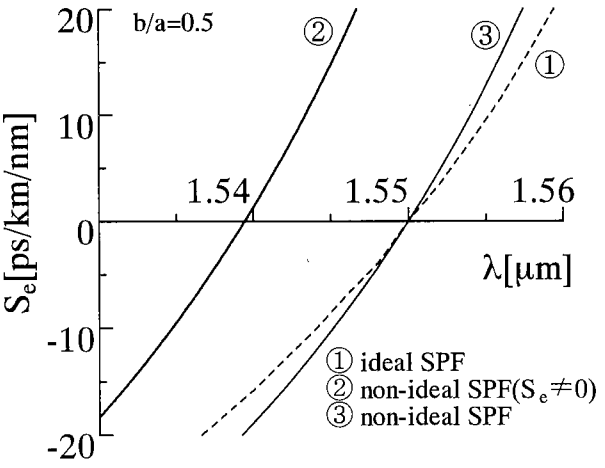

Fig.8 The total dispersion S_e versus wavelength λ

tion of round shoulder and fluctuations profile.

The non-ideal SPF was numerically analyzed by CFEM. So far, this method was not fully confirmed for an accuracy of propagation constants that were the most fundamental data for various propagation characteristic analyses of waveguides. For single elliptical core fiber, we compared propagation constants computed by CFEM with those computed by the rigorous analysis method using Mathieu functions. A good agreement of both results was found.

(Manuscript received January 29, 2001)

References

(1)M.J.Messerly, J.R.Onstott, and R.C.Mikkelson, A broadband single-polarization optical fiber, *J.Lightwave Technol.* vol.9, no.7, 817 (1991).

(2)T.Hinata, S.Furukawa, N.Namatame, and S.Nakajima, A single-polarization optical fiber of hollow pit type with zero total dispersion at wavelength of 1.55 μm , *J.Lightwave Technol.* vol.12, no.11, 1921 (1994).

(3)S.Furukawa, T.Tuneki, T.Hinata, and T.Hosono, Propagation characteristics of an elliptic optical fiber with pits outside an elliptical core, *IEE Technical Reports Japan*, EMT-96-112, 87 (1996).

(4)S.Furukawa, M.Shinohara, T.Hinata, and T.Hosono, Propagation characteristics of an elliptic optical fiber with pits alongside the major axis of an elliptic core, *IEE Technical Reports Japan*, EMT-97-54, 1997.

(5)S.Furukawa, T.Fujimoto, T.Hinata, and T.Hosono, Propagation characteristics of an elliptic optical fiber with triple-clad, *IEE Technical Reports Japan*, EMT-98-124, 131 (1998).

(6)S.Furukawa, K.Nakazawa, T.Hinata, and T.Hosono, The design method for triple clad silica core optical fibers with zero total dispersion at wavelengths of 1.3 μm and 1.55 μm, *IEICE*, vol.J69-C, no.11, 1411, (1986) (in Japanese).

(7)C.Vassallo, Circular fourier analysis of full Maxwell equations for arbitrary shaped dielectric waveguides — application to gain factors of semiconductor laser waveguides, *J.Lightwave Technol.*, vol.8, no.1, 1723 (1990).

(8)H.Etzkorn and W.E.Heinlein, Low-dispersion single mode silica fibre with undoped core and three F-doped claddings, *Electron. Lett.*, vol. 20, no. 10, 423 (1984).

(9)M.J.Adams, An introduction to optical waveguides , *John Wiley & Sons*, New York, 1981

Shinichi Furukawa (Non-member) was born in Kanagawa, Japan, on March 7, 1960. He received the B.S., M.S., and Ph.D. degree in electrical engineering from Nihon University, Tokyo, Japan, in 1982, 1984, and 1988, respectively.

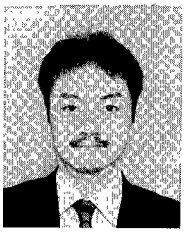

He worked at Amano Co., Ltd., Kanagawa, from 1984 to 1989 and Nihon University Junior College, Chiba, from 1989 to 1990. He is presently with Sano International Information Junior College, Tochigi, as a professor. His research interests are optical waveguide theory.

Dr. Furukawa is a member of the Institute of Electronics, Information and Communication Engineers of Japan.

Masayuki Saito (Non-member) was born in Saitama, Japan, on April 6, 1976. He received the B.S. and M.S. degree in electrical engineering from Nihon University, Tokyo, Japan in 1999 and 2001, respectively.

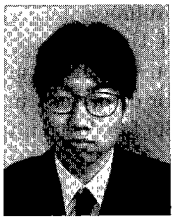

He is presently worked for Oki Electric Industry Co.,Ltd.. His research interests in University were optical waveguide theory.

Takashi Hinata (Member) received the B.S. degree from College of Science and Technology, Nihon University in 1958 and the Doctor of Engineering Degree from Nihon University in 1978. Since 1983, he has been a Professor at Nihon University. From 1988 to 1991, Dr. Hinata was the Chairman of the Technical Group on Electromagnetic Theory in the Institute of Electrical Engineers of Japan and the Institute of Electronics, Information and Communication Engineers. He has been been engaged in research on numerical analyses of optical waveguides, electromagnetic wave scattering and signal theory.